

*Letter to the Editor*

# ISO–SWS spectroscopy of IC443 and the origin of the IRAS 12 and 25 $\mu\text{m}$ emission from radiative supernova remnants\*

E. Oliva<sup>1</sup>, D. Lutz<sup>2</sup>, S. Drapatz<sup>2</sup>, and A.F.M. Moorwood<sup>3</sup><sup>1</sup> Osservatorio Astrofisico di Arcetri, Largo E. Fermi 5, I-50125 Firenze, Italy<sup>2</sup> Max-Planck-Institute für Extraterrestrische Physik, Postfach 1603, D-85740 Garching, Germany<sup>3</sup> European Southern Observatory, Karl-Schwarzschild-Strasse 2, D-85748 Garching bei München, Germany

Received 17 November 1998 / Accepted 3 December 1998

**Abstract.** ISO–SWS spectral observations of the supernova remnant IC443 are presented. Like other radiative SNRs, this object is characterized by prominent line–emitting filaments and relatively strong IRAS 12 and 25  $\mu\text{m}$  emission which is commonly interpreted as thermal radiation from very small grains stochastically heated by collisions with the hot plasma behind the shock front. This interpretation is challenged by the data presented in this *Letter* which indicate that most of the 12 and 25  $\mu\text{m}$  IRAS flux is accounted for by ionized line emission (mainly [NeII] and [FeII]). This result also seems to hold for other radiative SNRs. We also discuss the possible contribution of H<sub>2</sub> lines to the IRAS 12  $\mu\text{m}$  flux from the southern rim of IC443 and briefly analyze the element abundances derived from the observed ionic lines.

**Key words:** ISM: individual objects: IC443 – ISM: supernova remnants – infrared: ISM: lines and bands

## 1. Introduction

A significant fraction of the galactic supernova remnants were detected by the IRAS satellite (e.g. Arendt 1989, hereafter A89) and their relatively strong FIR emission has been normally interpreted as thermal radiation from dust which is heated by collisions with the hot (million degrees) plasma in the post–shock region (e.g. Braun & Strom 1986, Dwek et al. 1987). This emission could be an important cooling mechanism for non–radiative shocks in young SNRs (e.g. Ostriker & Silk 1973).

The spectral shape of the FIR emission reflects the temperature distribution of the dust which in turn depends on the shock speed and on the density, size and composition of the grains (e.g. Draine 1991). Young SNRs are expected to have a

*Send offprint requests to:* E. Oliva

\* Based on observations with ISO, an ESA project with instruments funded by ESA Member States (especially the PI countries: France, Germany, the Netherlands and the United Kingdom) and with the participation of ISAS and NASA. The SWS is a joint project of SRON and MPE.

FIR spectrum characterized by a single temperature because, in the hot ( $\gtrsim 2 \cdot 10^7$  K) plasma typical of these objects, the temperatures of collisionally heated dust grains approach the same value independent of grain size (e.g. Dwek 1987). This is in good agreement with the IRAS data of young SNRs (e.g. Cas A, Tycho, Kepler) whose spectral distributions are fairly well fitted by a single temperature blackbody (e.g. A89)

The IRAS colours of radiative SNRs are much more complex and require an ad hoc combination of dust components of different sizes and temperatures. In particular, the S(12)/S(25) IRAS colours are much bluer than those of young SNRs and require a very large population of very small ( $< 50 \text{ \AA}$ ) grains (e.g. Arendt et al. 1992). An alternative explanation is that the flux seen in the “blue” IRAS bands is dominated by line emission from the radiative filaments but this possibility could not be verified directly because of the difficulty of measuring the FIR lines prior to ISO. Attempts to estimate the line contamination by extrapolating optical spectral measurements using shock model predictions have led to contradictory conclusions (e.g. Mufson et al. 1986, Arendt et al. 1992).

In this *Letter* we present FIR spectral observations of a prototype radiative SNR which allow a direct comparison between the IRAS and line fluxes. The data are presented in Sect. 2, the results are discussed in Sect. 3 and in Sect. 4 we draw our conclusions.

## 2. Observations and results

A complete SWS01 (speed 4, 6700 sec total integration time) spectrum centered at  $\alpha=06^h 14^m 32^s .6$   $\delta=22^\circ 54' 05''$  (1950 coordinates) and roughly corresponding to position 1 of Fesen & Kirshner (1980) was obtained on October 16, 1997. The data were reduced using standard routines of the SWS interactive analysis system (IA) using calibration tables as of October 1998. Reduction relied mainly on the default pipeline steps, plus removal of signal spikes, elimination of the most noisy band 3 detectors, and flat–fielding. Note that SWS has a quite high spectral resolution ( $R = \lambda/\delta\lambda \simeq 1500$ ) and is not well suited for measurements of faint continuum fluxes. For the SWS01 mode,

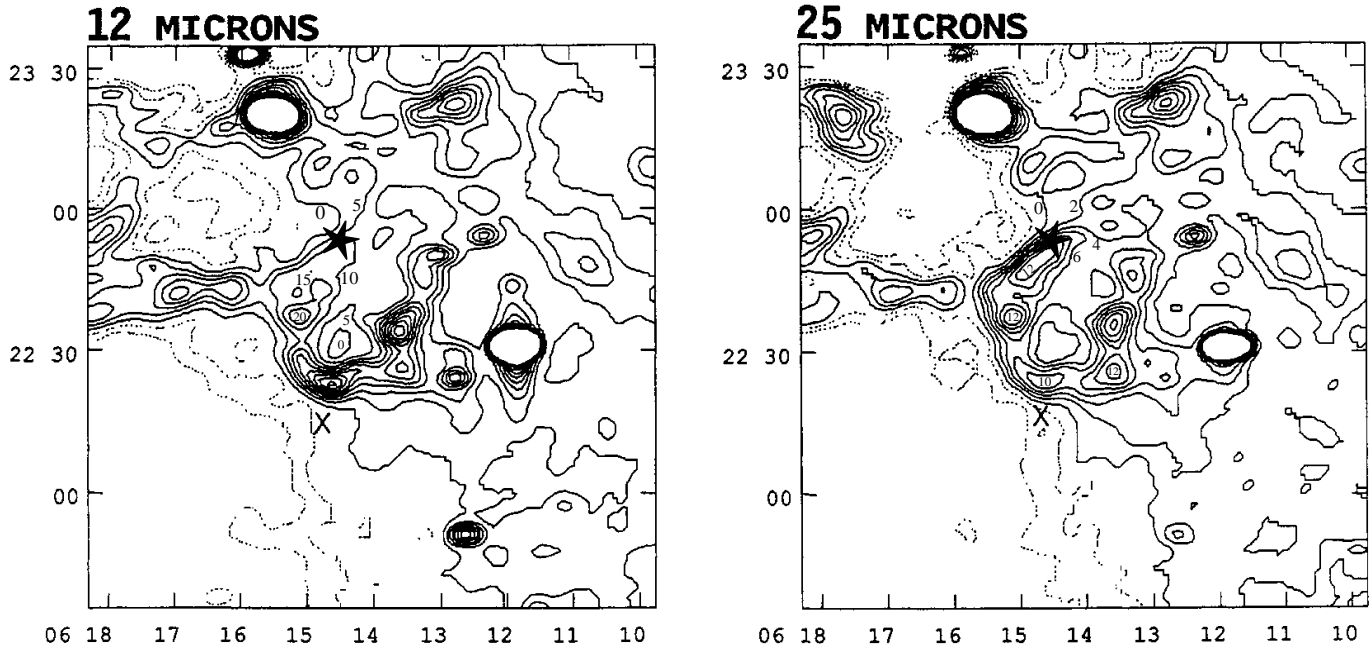


**Fig. 1.** The position of the SWS aperture (\*) is overlaid onto a reproduction of the IRAS maps of IC443 (adapted from Fig. 30a A89). The solid contours correspond to 0, 5, 10, 15, 20, 25, 30, 35, 40, 45 and 0, 2, 4, 6, 8, 10, 12, 14, 16, 18 ( $\times 10^{-8} \text{ W m}^{-2} \text{ sr}^{-1}$ ) in the 12 and 25  $\mu\text{m}$  bands, respectively. Note that the size of the SWS aperture is much smaller than the symbol used to mark its position.

**Table 1.** Observed ISO line fluxes

| Line                              | Flux <sup>(1)</sup> | Slit <sup>(2)</sup> | $\Sigma$ -IRAS <sup>(3)</sup> |                  |                  |
|-----------------------------------|---------------------|---------------------|-------------------------------|------------------|------------------|
|                                   |                     |                     | 12 $\mu\text{m}$              | 25 $\mu\text{m}$ | 60 $\mu\text{m}$ |
| [NeII] $\lambda$ 12.81            | 18 (3)              | 14 $\times$ 27      | 20                            | –                | –                |
| [NeIII] $\lambda$ 15.56           | 10 (2)              | 14 $\times$ 27      | –                             | –                | –                |
| [FeII] $\lambda$ 17.93            | 4 (1)               | 14 $\times$ 27      | –                             | 2                | –                |
| [SiII] $\lambda$ 18.71            | 4 (2)               | 14 $\times$ 27      | –                             | 3                | –                |
| [OIV] $\lambda$ 25.88             | 3 (1)               | 14 $\times$ 27      | –                             | 3                | –                |
| [FeII] $\lambda$ 25.98            | 8 (1)               | 14 $\times$ 27      | –                             | 10               | –                |
| [SiII] $\lambda$ 34.8             | 52 (7)              | 20 $\times$ 33      | –                             | –                | 2                |
| Observed IRAS fluxes <sup>a</sup> |                     |                     | 10                            | 10               | 60               |

(1) Observed line flux, units of  $10^{-16} \text{ W m}^{-2}$ , errors are given in parenthesis

(2) Size (in arcsec) of the SWS apertures

(3) Equivalent surface brightness in the IRAS bands, units of  $10^{-8} \text{ W m}^{-2} \text{ sr}^{-1}$

<sup>a</sup> Observed IRAS surface brightness at the position of the SWS aperture, estimated from Fig. 30a of A89, see also Fig. 1.

in particular, *s/n* and detector drifts between dark current measurements do not allow measurements of continuum emission at levels much below 1 Jy. The measured IRAS 12 and 25  $\mu\text{m}$  “continuum” fluxes from the SNR would correspond to only  $\approx 0.01$  Jy in the SWS aperture and cannot therefore be detected with the spectral observations presented here.

The spectral sections including well detected lines are displayed in Fig. 2 and the derived line fluxes are listed in Table 1 together with their contribution to the IRAS fluxes, estimated using the spectral response shown in Fig. 3. The line profiles

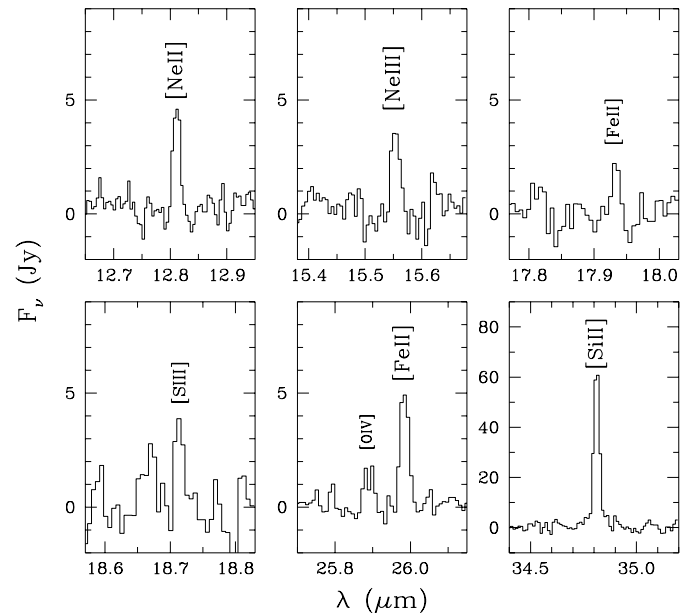


**Fig. 2.** Selected sections of the SWS01 spectrum of the north-east rim of IC443, note that each spectral segment has been “continuum subtracted” (using a  $\leq 2$  degree polynomial) to remove instrumental offsets and drifts. The position of instrument aperture is shown in Fig. 1.

are not resolved within the noise (i.e.  $\text{FWHM} < 400 \text{ km/s}$ ), and their centroids are not significantly red/blue-shifted.

The most striking result is that the surface brightness of [NeII] $\lambda$ 12.8 alone is *larger* than that observed by IRAS through the 12  $\mu\text{m}$  filter. This apparent contradiction reflects the somewhat higher spatial resolution of ISO-SWS relative to the un-

dersampled IRAS maps. More specifically, the line emitting filaments visible in the  $H\alpha$  and [SII] images of Mufson et al. (1986) are quite uniformly distributed over many arcmin, i.e. an area larger than the IRAS map resolution, and the average line surface brightness over this area is roughly a factor of 2–4 lower than that within the ISO–SWS aperture. In other words, the ISO spectra, although centered on a bright optical filament, does not sample a spot of exceptionally large line surface brightness, but rather a “typical” line emitting region.

This indicates, therefore, that the IRAS 12  $\mu\text{m}$  “continuum” is indeed dominated by [NeII] line emission, i.e. that this line accounts for at least 50% of the observed IRAS flux. A similar reasoning applies to the IRAS 25  $\mu\text{m}$  flux which is strongly contaminated by emission in the [FeII] $\lambda$ 26.0 ground state transition plus significant contribution from [OIV] $\lambda$ 25.9, [SIII] $\lambda$ 18.7 and [FeII] $\lambda$ 17.9 (cf. Table 1).

Another interesting result is that [FeII] $\lambda$ 26.0/[NeII] $\lambda$ 12.8 and [FeII] $\lambda$ 26.0/[SiII] $\lambda$ 34.8 are both a factor of  $\approx 1.7$  lower than those observed in RCW103 (Oliva et al. 1998), while the density sensitive [FeII] $\lambda$ 17.9/ $\lambda$ 26.0 ratio is similar in the two objects. This result indicates that IC443 has a lower Fe gas phase abundance than RCW103 where the Fe/Ne and Fe/Si relative abundances were found to be close to their solar values. This difference may reflect intrinsic differences in the ISM total element abundances or, more likely, imply that the shock in IC443 is slower and therefore less effective in destroying the Fe-bearing grains. This last possibility is also supported by other “speedometers”, i.e. the line surface brightness and the [NeIII]/[NeII] ratio which are lower by a factor of 7 and 1.6, respectively.

### 3. Discussion

The data presented above strongly suggest that most of the 12 and 25  $\mu\text{m}$  flux from the NE rim of IC443 is due to ionic line emission rather than continuum emission from warm dust. We address here the following questions. Can this result be generalized to other radiative SNRs? Are there other lines which may severely contaminate IRAS measurements of this and other remnants?

#### 3.1. The IRAS 12 and 25 $\mu\text{m}$ emission from other SNRs

The easiest and most direct estimate of the line contribution to the IRAS fluxes requires a measurement of the FIR line intensity from the whole SNR. This is virtually impossible in IC443 and other radiative remnants in the Galaxy because of their very large projected sizes, but is feasible in the LMC where e.g. the remnant N49 has been mapped with SWS by Oliva et al. (in preparation). They find a total [NeII] $\lambda$ 12.8 line intensity of  $2 \cdot 10^{-14} \text{ W m}^{-2}$  and equal, within the errors, to the  $F(12\mu\text{m})=2.2 \cdot 10^{-14} \text{ W m}^{-2}$  IRAS flux reported by Graham et al. (1987).

For remnants where direct measurements of FIR lines is not available, a reasonable estimate of their fluxes can be obtained by scaling optical line measurements using available ISO spectral observations of radiative SNRs, namely IC443 (this paper),

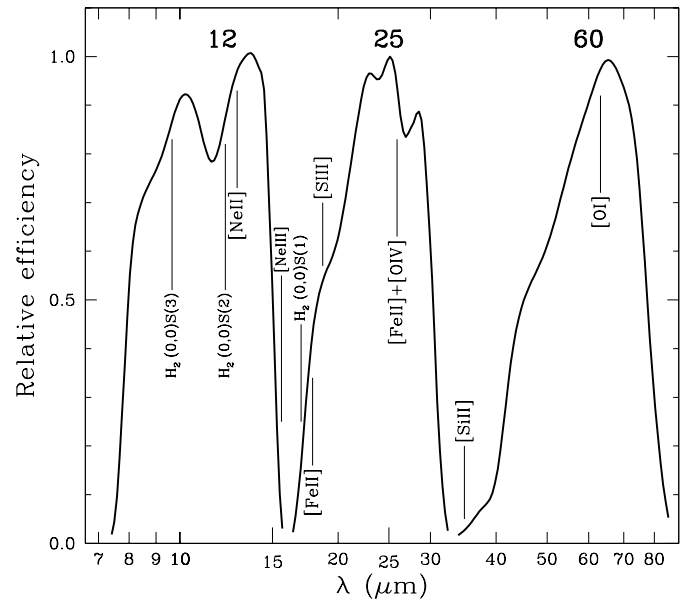


**Fig. 3.** Instrumental spectral response of IRAS (adapted from Fig. 2 of Neugebauer et al. 1984) with overlaid the positions of the brightest ionic, atomic and molecular lines.

RCW103 (Oliva et al. 1998) and N49 (Oliva et al. in preparation). These indicate that the [NeII] and [FeII]+[SIII]+[OIV] line contribution to the 12 and 25  $\mu\text{m}$  filters are both roughly equal to the flux of  $H\beta$ . Unfortunately, relatively few optical spectrophotometric observations of SNRs are available in the literature and are altogether missing for several important radiative remnants such as W44 and W49B. Nevertheless, the SW filament of RCW86 has  $\Sigma(H\beta) \approx 4 \cdot 10^{-7}$  (Leibowitz & Danziger 1983) and very similar to the  $\Sigma \approx 3 \cdot 10^{-7} \text{ W m}^{-2} \text{ sr}^{-1}$  IRAS 12 and 25  $\mu\text{m}$  fluxes found by A89. Similarly, the NE filament of the Cygnus Loop has  $\Sigma(H\beta) \approx 1 \cdot 10^{-7}$  (Fesen et al. 1982) and close to the IRAS surface brightness  $\Sigma \approx 8 \cdot 10^{-8} \text{ W m}^{-2} \text{ sr}^{-1}$  (A89). These results suggest, therefore, that lines account for most of the IRAS 12 and 25  $\mu\text{m}$  emission from line emitting filaments of radiative SNRs.

Another interesting exercise is to compare optical line and IRAS fluxes in a younger remnant such as the Kepler SNR for which accurate line photometric measurements are available (D’Odorico et al. 1986). The total  $H\beta$  emission from the whole remnant is  $2.9 \cdot 10^{-15} \text{ W m}^{-2}$  and only 2% and 0.6% of the IRAS flux in the 12 and 25  $\mu\text{m}$  bands, respectively. This indicates, therefore, that line contamination is negligible in this object.

#### 3.2. Contamination from other lines

The positions of the most important lines are marked in Fig. 3 where one can see that [SiII] $\lambda$ 34.8, although very prominent in SNRs, does not contribute significantly because it falls at a wavelength where IRAS was virtually blind. The same applies to [NeIII] $\lambda$ 15.6 which has an intensity comparable to [NeII] but falls in the hole between the 12 and 25  $\mu\text{m}$  filters.

The possible contribution of [OI] $\lambda$ 63.0 to the IRAS 60  $\mu\text{m}$  band was already pointed out by Burton et al. (1990) who observed this line in the southern (“molecular”) rim of IC443 using a 33” aperture spectrometer on the KAO and found line surface brightnesses a factor of  $\sim 2$  larger than those measured by IRAS. On the other hand, however, ISO–LWS measurements of [OI] $\lambda$ 63.0 through a  $\phi$  80” aperture centered on the optical filaments of W44 (Reach & Rho 1996) yield a line surface brightness a factor of  $\sim 2.5$  lower than the IRAS 60  $\mu\text{m}$  flux<sup>1</sup> indicating, therefore, that the contamination by [OI] is relatively unimportant, at least in this remnant.

The H<sub>2</sub> rotational lines could strongly affect the 12  $\mu\text{m}$  band and may explain why the S(12)/S(25) ratio is a factor of  $\sim 2.5$  larger on the southern rim of IC443, i.e. at  $\approx 06^{\text{h}}14^{\text{m}}40^{\text{s}}+22^{\circ}23'$  (cf. Fig. 1). This region is a well known powerful source of H<sub>2</sub> (1,0)S(1) $\lambda$ 2.12 line emission (Burton et al. 1988) whose spatial distribution closely resembles the IRAS 12  $\mu\text{m}$  contours. Ground-based observations of the (0,0)S(2) $\lambda$ 12.3 rotational transition were obtained by Richter et al. (1995) who measured a line flux  $\approx 10$  times brighter than (1,0)S(1) $\lambda$ 2.12. Assuming a constant I( $\lambda$ 12.3)/I( $\lambda$ 2.12) ratio over the large area mapped in the latter transition by Burton et al. (1988) yields an average line surface brightness of about  $1.5 \cdot 10^{-7} \text{ W m}^{-2} \text{ sr}^{-1}$  or 1/3 of the IRAS 12  $\mu\text{m}$  peak surface brightness. Considering that the H<sub>2</sub> spectrum of IC443 is remarkably similar to that of Orion peak 1 (e.g. Richter et al. 1995) one then expects similar fluxes in the (0,0)S(3) $\lambda$ 9.66 and (0,0)S(2) $\lambda$ 12.3 lines (Parmar et al. 1994) or, equivalently, that the two lines should account for about 2/3 of the IRAS 12  $\mu\text{m}$  flux.

Finally, it should be noted that IRAS was virtually blind to the H<sub>2</sub>(0,0)S(1) $\lambda$ 17.0 line (cf. Fig. 3) while the highly forbidden ground state transition (0,0)S(0) $\lambda$ 28.2 is most probably too weak to significantly contaminate the 25  $\mu\text{m}$  IRAS band (cf. e.g. Fig. 2 of Oliva et al. 1998).

#### 4. Conclusions

An ISO–SWS spectrum of IC443 has revealed prominent [NeII] and [FeII] line emission which, together with [SIII] and [OIV], account for most of the observed IRAS flux in the 12, 25  $\mu\text{m}$  bands. Simple arguments indicate that this is probably the case in other radiative SNRs and this result suggests that the unusually blue IRAS colours of radiative SNRs simply reflect line contamination, rather than a large population of small grains which are otherwise required to explain the warmer “continuum” emission. Available ground based data also indicate that S(2), S(3) rotational lines of H<sub>2</sub> contribute to a large fraction of the IRAS 12  $\mu\text{m}$  emission from the southern rim of IC443.

The relative fluxes of the ionic lines detected by ISO yield a  $\approx 0.6 \times$  solar Fe gas–phase relative abundance which is significantly lower than that found in the much more powerful RCW103 supernova remnant. This may imply that the shock in IC443 is slower and thus less effective in destroying the Fe-bearing grains. This scenario is also supported by the lower line surface brightness and [NeIII]/[NeII] ratio which both indicate a lower shock speed in IC443.

*Acknowledgements.* We thank the referee, R. Arendt, for useful comments and criticisms. E. Oliva acknowledges the partial support of the Italian Space Agency (ASI) through the grant ARS–98–116/22. SWS and the ISO Spectrometer Data Center at MPE are supported by DLR (formerly DARA) under grants 50–QI–8610–8 and 50–QI–9402–3.

#### References

- Arendt R.G., 1989, *ApJS* 70, 1 (A89)  
 Arendt R.G., Dwek E., Leisawitz D., 1992, *ApJ* 400, 562  
 Braun R., Strom R.G., 1986, *A&A* 164, 193  
 Burton M.G., Geballe T.R., Brand P.W.J.L., Webster A.S., 1988 231, 617  
 Burton M.G., Hollenbach D.J., Haas M.R., Erickson E.F., 1990, *ApJ* 355, 197  
 D’Odorico S., Bandiera R., Danziger I.J., Focardi P., 1986, *AJ* 91, 1382  
 Dwek E., 1987, *ApJ* 322, 812  
 Dwek E., Petre R., Szymkowiak A., Rice W.L., 1987, *ApJL* 320, L27  
 Draine B.T., 1981, *ApJ* 245, 880  
 Fesen R.A., Kirshner R.P., 1980, *ApJ* 242, 1023  
 Fesen R.A., Blair W.P., Kirshner R.P., 1982, *ApJ* 262, 171  
 Graham J.R., Evans A., Albinson J.S., Bode M.F., Meikle W.P.S., 1987, *ApJ* 319, 126  
 Leibowitz E.M., Danziger I.J., 1983, *MNRAS* 204, 273  
 Mufson S.L., McCollough M.L., Dickel J.R., Petre R., White R., Chevalier R., 1986, *AJ* 92, 1349  
 Neugebauer G., Habing H. J., van Duinen R., Aumann H. H., Baud B., Beichman C. A., Beintema D. A., Boggess N., Clegg P. E., de Jong T., Emerson J. P., Gautier T. N., Gillett F. C., Harris S., Hauser M. G., Houck J. R., Jennings R. E., Low F. J., Marsden P. L., Miley G., Olon F. M., Pottasch S. R., Raimond E., Rowan-Robinson M., Soifer B. T., Walker R. G., Wesselius P. R., Young E., 1984, *ApJL* 278, L1  
 Oliva E., Moorwood A.F.M., Drapatz S., Lutz D., Sturm E., 1998, submitted to *A&A*  
 Ostriker J.P., Silk J., 1973, *ApJL* 184, L113  
 Parmar P.S., Lacy J.H., Achtermann J.M., 1994, *ApJ* 430, 786  
 Reach W.T., Rho J., 1996, *A&A* 315, L277  
 Richter M.J., Graham J.R., Wright G.S., Kelly D.M., Lacy J.H., 1995, *ApJL* 449, L83

<sup>1</sup> Note that the “continuum” in the LWS spectra of W44 by Reach & Rho (1996) is most probably an instrumental artifact, its level being 10 times brighter than the IRAS 60  $\mu\text{m}$  background+source flux